J Sol-Gel Sci Technol (2015) 73:103–111
DOI 10.1007/s10971-014-3500-8

ORIGINAL PAPER

Hierarchically organized silica monoliths: influence of different acids on macro- and mesoporous formation

Sylvia Flaig · Johanna Akbarzadeh · Herwig Peterlik · Nicola Hüsing

Received: 23 June 2014 / Accepted: 7 September 2014 / Published online: 23 September 2014

Abstract The influence of different acids, such as hydrochloric acid, sulfuric acid, nitric acid, hydrobromic acid and acetic acid on the polymerization-induced phase separation process in the formation of hierarchically organized silica monoliths was investigated in detail. Special emphasis is given to systems synthesized from tetrakis(2-hydroxyethoxy)silane (EGMS) or tetramethoxysilane (TMOS) as the silica source in the presence of Pluronic® P123 serving as structure-directing agent. The obtained silica monoliths exhibited a co-continuous and cellular macroporous structure comprising 2D hexagonally arranged mesopores with high specific surface areas ranging from 320–787 $m^2 g^{-1}$ independent of the applied silane precursor and regardless whether hydrochloric acid or sulfuric acid was used. A drastic change in macropore morphology to closed pores or particulate structures was observed for nitric, bromic as well as acetic acid. For sulfuric and nitric acid, the influence on the mesostructure was not as pronounced and 2D hexagonally arranged mesopores were obtained. With bromic and acetic acid a loss in mesopore ordering has been observed. Best developed hierarchically organized networks with respect to a co-continuous, cellular macroporous network, specific surface area and 2D hexagonally arranged mesopores were obtained for EGMS as well as for TMOS with P123 in sulfuric acid.

Keywords Silica · Sol–gel · Acid · Macro-/mesoporous · Monolith

1 Introduction

Hierarchically organized silica monoliths with pore dimensions covering the nm- up to the μm-range or even larger have been investigated in materials science for the last decades. Applications range from chromatographic supports and catalysts to adsorbents, for which an interconnected, well-defined porosity in the microporous (<2 nm), mesoporous (2–50 nm) to macroporous (>50 nm) regime is desired [1]. Mesopores lead to size or shape selectivity and high specific surface areas, while macropores enable efficient mass transport to the active sites. For designing those well-defined pore structures different approaches, such as hard or soft templating, which can be applied during sol–gel processing, were developed [2–12].

Hierarchically organized (hybrid organo-) silica monoliths with well-ordered 2D hexagonally arranged mesopores and a co-continuous macropore network have been reported by Nakanishi et al. [13]. In their work, tetramethoxysilane (TMOS) or bridged organobissilyl-species were processed in nitric acid with a small amount of P123 as surfactant resulting in a filigree macroporous network comprising periodically arranged mesopores. Another approach towards cellular macroporous silica monoliths with well-organized, 2D hexagonally arranged mesopores has been presented by the application of glycol- or polyol-modified silanes in the presence of P123 in hydrochloric acid [14–16].

Electronic supplementary material The online version of this article (doi:10.1007/s10971-014-3500-8) contains supplementary material, which is available to authorized users.

S. Flaig · N. Hüsing (✉)
Materials Chemistry, Paris-Lodron University Salzburg, Hellbrunnerstrasse 34, 5020 Salzburg, Austria
e-mail: nicola.huesing@sbg.ac.at

J. Akbarzadeh · H. Peterlik
Faculty of Physics, University of Vienna, Strudlhofgasse 4, 1090 Vienna, Austria

For most sol-gel reactions an acidic or basic catalyst has been applied. However, it seems that for fabricating silica materials the applied acid in each synthesis procedure is chosen rather randomly. Some groups seem to prefer hydrochloric acid, others nitric acid, and several procedures relied on acetic acid; In some cases even synthesis procedures containing an acid/acid two-step process with hydrochloric acid and nitric acid have been reported [17]. Investigations on hydrolysis and condensation behavior of TEOS using different acids (HF, HCl, HNO_3, H_2SO_4, CH_3COOH or NH_4OH) showed that the rate and extent of hydrolysis was most influenced by the strength and concentration of the acid catalyst, whereas temperature and solvent were of secondary importance [18]. In the synthesis of SBA-15 materials an influence on meso- and macrostructure due to the application of different acids (HCl, H_2SO_4, HNO_3, H_3PO_4, HBr) was reported previously [19, 20]. To shed more light on the role of the acid in the polymerization-induced phase separation process we investigated the impact of different acids, such as hydrochloric acid, sulfuric acid, nitric acid, hydrobromic acid and acetic acid, on the structure formation of silica monoliths.

These silica monoliths were on the one hand based on a synthesis procedure with tetrakis(2-hydroxyethoxy)silane (EGMS) and P123 and on the other on a procedure by Nakanishi et al. [13] where TMOS and P123 were used for synthesis. The alteration of the macroporous structure, mesopore arrangement, porosity as well as lattice parameters of the regular pore arrangement in dependence of the different acids was investigated by SEM, SAXS and nitrogen sorption measurements.

2 Materials and experimental

2.1 Precursor and gel synthesis

Tetramethoxysilane (TMOS, M = 152.22 g mol^{-1}) and the block copolymer Pluronic® P123 (M ~5,800 g mol^{-1}) were purchased from Sigma-Aldrich and were used without further purification. Tetraethyl orthosilicate (TEOS, M = 208.32 g mol^{-1}) and ethylene glycol (EG, M = 62.07 g mol^{-1}) were purchased from Merck. Ethylene glycol was dried over anhydrous sodium sulfate and distilled from magnesium. The applied mineral acids, such as hydrochloric acid (32 wt%), nitric acid (65 wt%), hydrobromic acid (32 in 68 wt% acetic acid resulting in concentrations of 1 mol L^{-1} HBr and 2.8 mol L^{-1} CH_3COOH), and sulfuric acid (95–97 wt%) were purchased from VWR-Prolabo or Merck and diluted to 1 mol L^{-1}. Acetic acid (100 %, Merck) was diluted to 2.8 mol L^{-1} (pH = 1.5) comparable to the acetic acid content in the HBr solution.

2.1.1 Tetrakis(2-hydroxyethoxy)silane (EGMS)

The synthesis of EGMS was performed according to Mehrotra and Narain with some modifications in the transesterification reaction as published by Brandhuber et al. [15, 21, 22].

2.1.2 Gel synthesis

The surfactant, Pluronic® P123, was dissolved in the particular acid with a ratio of P123/acid = 20/80 wt% for EGMS, and P123/acid = 4.5/95.5 wt% when TMOS was used as precursor. The composition of the sol was Si/P123/acid = 8.4/20/80 wt% when EGMS was applied. Using 3 g of the surfactant solution (20/80 wt% meaning 0.6 g P123 and 2.4 g of the respective 1.0 M acid) resulted in 2.6 g (9.0 mmol Si, 8.4 wt% Si) EGMS. This mass might change depending on the ceramic yield of SiO_2 in EGMS. In our case, the ceramic yield of 20.7 % SiO_2 was determined for EGMS by thermogravimetric analyses. The amount and ratios for the materials synthesized with TMOS were adapted from the procedure described by the group of Nakanishi with Si/P123/acid = 0.06/4.5/95.5 wt%, with a reduced gelation temperature of 40 °C [13]. Here, 0.35 g TMOS (2.3 mmol) were homogenized with 6 g of the surfactant solution (4.5/95.5 wt%) at 0°C–RT. For both procedures, the resulting sol was poured into molds and kept 7 day at 40 °C for gelation and aging. After aging, the gels were washed three times with ethanol, dried with supercritical carbon dioxide and calcined at 200 °C (0.2 °C min^{-1}) [23, 24].

2.2 Characterization

2.2.1 Small angle X-ray scattering (SAXS)

SAXS measurements were performed using a laboratory X-ray source (Bruker Nanostar) with a rotating copper anode generator together with a 2D position sensitive detector (Våntec 2000, gas detector with microgap technology). The monolithic samples were ground to powders and attached between two strips of Scotch™ tape. The scattering patterns were radially averaged and corrected for background scattering in order to obtain the scattering intensity in dependence on the scattering vector $q = 4\pi\sin(\theta)/\lambda$, where 2θ is the scattering angle and $\lambda = 0.1542$ nm the X-ray wavelength. Parameters, such as d-spacing d_{10} and lattice constant a, were calculated with $d_{10} = 2\pi/q_{10}$ and $a = 2d_{10}/\sqrt{3}$ for a 2D hexagonal lattice [25]. The measurements were carried out in transmission at the sample to detector distance of 108 cm giving access to a q-range of 0.1–2.8 nm^{-1}.

2.2.2 Scanning electron microscopy (SEM)

For scanning electron microscopy (SEM) images monolithic pieces sputtered with gold for 120 s were analyzed with a Stereoscan 430, Zeiss Leo 438 VP and a Zeiss FE-SEM Ultraplus operating at 5–10 kV.

2.2.3 Nitrogen sorption measurements

From nitrogen adsorption/desorption measurements specific surface areas and pore size distributions were calculated. Isotherms were recorded on an ASAP2420 (Micromeritics) at 77 K. All samples were degassed at 100 °C for 3 h prior to the measurements. A BET calculation in a relative pressure range from 0.05 to 0.3 p/p^0 led to the specific surface areas [26]. Furthermore, pore size distributions were determined by the BJH method from the adsorption branches of the isotherms [27].

3 Results and discussion

In this work, the influence of different acids on the pore formation in silica monoliths bearing a bimodal pore size distribution is investigated. Sol-gel processing was performed with acids in concentrations of 1.0 M, for which the silica surface is positively charged (PZC $\sim$2). Applying non-ionic surfactants, such as P123, the mechanism for the interactions between the inorganic matrix (I^+), the non-ionic surfactant (S^0) and the anion (X^-) of the applied acid can be presented by $(S^0H^+)(X^-I^+)$ as reported by Zhao et al. [28]. Solubilization of the non-ionic poly(alkylene oxide) surfactant is favored due to the association of hydronium ions (H^+) with the oxygen atoms of the surfactant (S^0). In this $(S^0H^+)(X^-I^+)$ mechanism, the anion acts as a mediator between the positively charged silica species and the surfactant, where the electronegativity, radius, charge and polarizability of the anion presumably plays an important role. For this reasons a strong impact on macro- and mesopore formation is expected, when the different acids are applied. Hydrochloric acid ($pK_a = -8.0$), sulfuric acid ($pK_a = -3.0$; 1.99), nitric acid ($pK_a = -1.3$), and hydrobromic acid ($pK_a = -9.0$) are all classified as very strong acids with pK_a-values <0 [29]. As a reference, because the applied hydrobromic acid contained acetic acid for stabilization, acetic acid with a pK_a-value of 4.76 was also applied [29].

Silica monoliths were prepared by applying the two different silica precursors EGMS, with a glycol to silicon ratio of 4:1, and TMOS. While TMOS is a chemically well-defined silane precursor, EGMS is composed of monomers, bridging and chelating Si-species, which are in a dynamic equilibrium with free ethylene glycol [21]. For hydrolysis, the aqueous acids HCl, H_2SO_4, HNO_3, HBr or CH_3COOH were used. As expected, samples prepared with EGMS showed shorter gelation times for all acids when compared to TMOS-based monoliths. This can be explained by the instantaneous hydrolysis reaction of EGMS in water resulting in gel times that are only governed by the condensation reaction, but is also expected due to the lower concentration of TMOS compared to EGMS, also resulting in lower densities (see vide infra). Hydrolysis of TMOS in acidic media is delayed and thus the supply of hydrolyzed species is one of the rate limiting steps for the gelation [18]. The samples prepared with EGMS showed gelation times from 45 min for HCl up to 85 min for HNO_3, which can be assumed as a result of a decrease in acidic strength. Further increase in gelation time (95 min) was observed for HBr. All EGMS-based samples resulted in transparent gels and after 1–3 h phase separation occurred and mechanically stable, white monoliths were obtained (Table 1). For the TMOS derived monoliths gelation and phase separation occurred simultaneously after 1 h when hydrochloric acid was used. With nitric acid or hydrobromic acid gelation took much longer and was difficult to detect because very weak and jelly-like monoliths were formed. Previous experiments with TEOS using different acids for hydrolysis and condensation showed no major influence on the gelation time, when strong acids, such as HCl, HNO_3 or H_2SO_4 were applied [18]. In general, rate and extent of hydrolysis was mostly influenced by the strength (strong or weak acid) and concentration of the acid catalyst, whereas temperature and solvent were of secondary importance. Moreover, nucleophilic, electronegative and non-polarisable anions may be coordinated directly to the silicon atom resulting in an expansion of the coordination sphere [18]. Therefore, a decrease in reaction rate and accordingly an increase in gelation time can be expected for halides in the following order $F^- < Cl^- < Br^-$ and the shorter gelation times with HCl compared to HBr can be explained.

Both silica precursors EGMS and TMOS resulted in white monoliths for all acids after aging. After drying with supercritical carbon dioxide and calcination at 200 °C the materials synthesized with EGMS resulted in white and rigid monoliths with a theoretical bulk density of 0.1 g cm^{-3}. In contrast, white and fragile materials were obtained by applying TMOS as silica precursor, where weak monoliths could be obtained when hydrochloric acid or sulfuric acid was used and only monolithic pieces resulted for nitric, hydrobromic and acetic acid (see Fig. 1). The TMOS recipe with lower silica and higher water content compared to the monoliths derived from EGMS resulted in very low theoretical densities of 0.02 g cm^{-3}, which is responsible for the fragile morphology of the materials. Furthermore, the stiff network obtained from EGMS showed a relatively low shrinkage of $\sim$10 %,

Table 1 Gelation time, specific surface area (obtained from nitrogen sorption), first scattering peak position q_{10} (obtained from SAXS), and resultant morphology of the silica samples prepared with the various acids

Sample	Gelation time/min	$S_{spec}/m^2\ g^{-1}$	q_{10} (error ± 0.02/nm^{-1})	Morphology	
				µm-range	mm-range
EGMS/P123/HCl	45	464	0.68	Co-continuous	Rigid monolith
EGMS/P123/H_2SO_4	—[a]	641	0.67	Co-continuous	Rigid monolith
EGMS/P123/HNO_3	85	373	0.69	Isolated pores	Rigid monolith
EGMS/P123/HBr	95	524	0.70	Co-continuous	Rigid monolith
EGMS/P123/CH_3COOH	—[a]	634	0.75	Isolated pores	Rigid monolith
TMOS/P123/HCl	60	320	0.78	Co-continuous	Fragile monolith
TMOS/P123/H_2SO_4	—[a]	787	0.72	Co-continuous	Fragile monolith
TMOS/P123/HNO_3	2,880	451	0.74	Particulate	Monolithic pieces
TMOS/P123/HBr	2,880	882	0.88	Particulate	Monolithic pieces
TMOS/P123/CH_3COOH	—[a]	584	0.77	Isolated pores	Monolithic pieces

[a] Gelation time was not detected

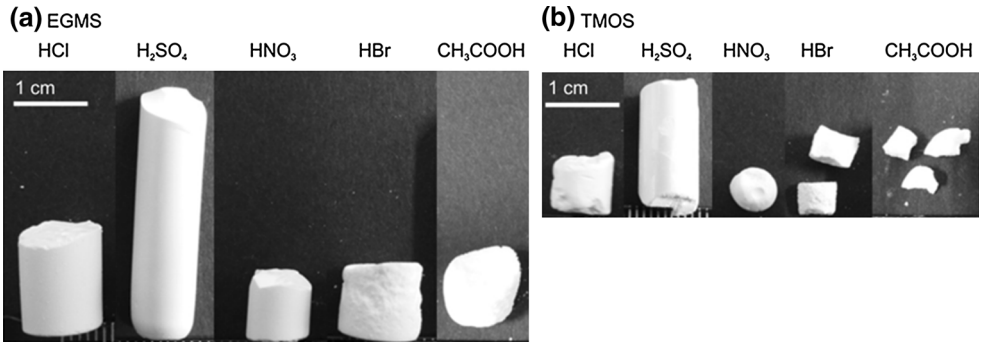

Fig. 1 Photographs of the silica monoliths from EGMS (**a**) and TMOS (**b**)

whereas for the monoliths derived from TMOS shrinkages of 20–25 % were observed.

From a chemical point of view, sol-gel processing of alkoxysilanes results in the release of alcohols or diols during the evolution of the 3D gel network. Numerous parameters influence network development and formation: (1) the applied precursor and its amount, (2) an increase in acid concentration accelerates the reaction rate and can lead to a collapse of the mesopore arrangement, (3) generated alcohols/polyols during hydrolysis influence the formation of surfactant arrays in the sol and therefore, mesopore arrangement in the final materials as well as (4) an increase in temperature leads to a decrease in the arrangement of the liquid crystalline phase and an increase in reaction rate of the precursor [21, 30, 31].

Nakanishi et al. published the synthesis of hierarchically organized silica monoliths with a well-defined macro- and mesostructure based on TMOS with nitric acid and P123 at 60 °C [13]. Variation of the water content has shown that a large excess of water (water/Si > 100) resulted in a cellular and uniform macrostructure with strands of 0.4–0.8 µm in diameter and 2–5 µm in length. Moreover, a highly porous network (V_{max} = 600–700 $cm^3\ g^{-1}$) with 2D hexagonally arranged mesopores was achieved. A reduction of the water content to water/Si = 11/1 leads to coarser structures in the µm-regime, lower pore volumes (V_{max} ~300 $cm^3\ g^{-1}$) and a loss of the long range order of the mesopores. In the present work a lower gelation and aging temperature of 40 °C has been applied, resulting in comparable porous architectures with a cellular network in the µm-range only for the sample TMOS/P123/HCl (Fig. 2f). With HNO_3 at 40 °C a particulate structure with spherical particles up to 10 µm in size is obtained (Fig. 2h). Just for comparison, silica monoliths prepared from alkoxysilanes (tetramethoxy- and tetraethoxysilanes) with processing parameters similar to the EGMS-based samples (ρ = 0.1 g cm^{-3}, P123/ 1 M HCl = 20/80 wt%) resulted in porous materials with a particulate macrostructure and no visible mesopore order. In Fig. 2 the SEM images of all samples are presented and it is clearly visible that not only the choice of acid, but also the choice of silica precursor has a very strong impact on the macropore morphology. Using EGMS as the silica source, a cellular network with strands of 1–2 µm in length and 0.2–0.4 µm in diameter is formed if hydrochloric or sulfuric acid are used (Fig. 2a, b). A change in macropore morphology to isolated pores with

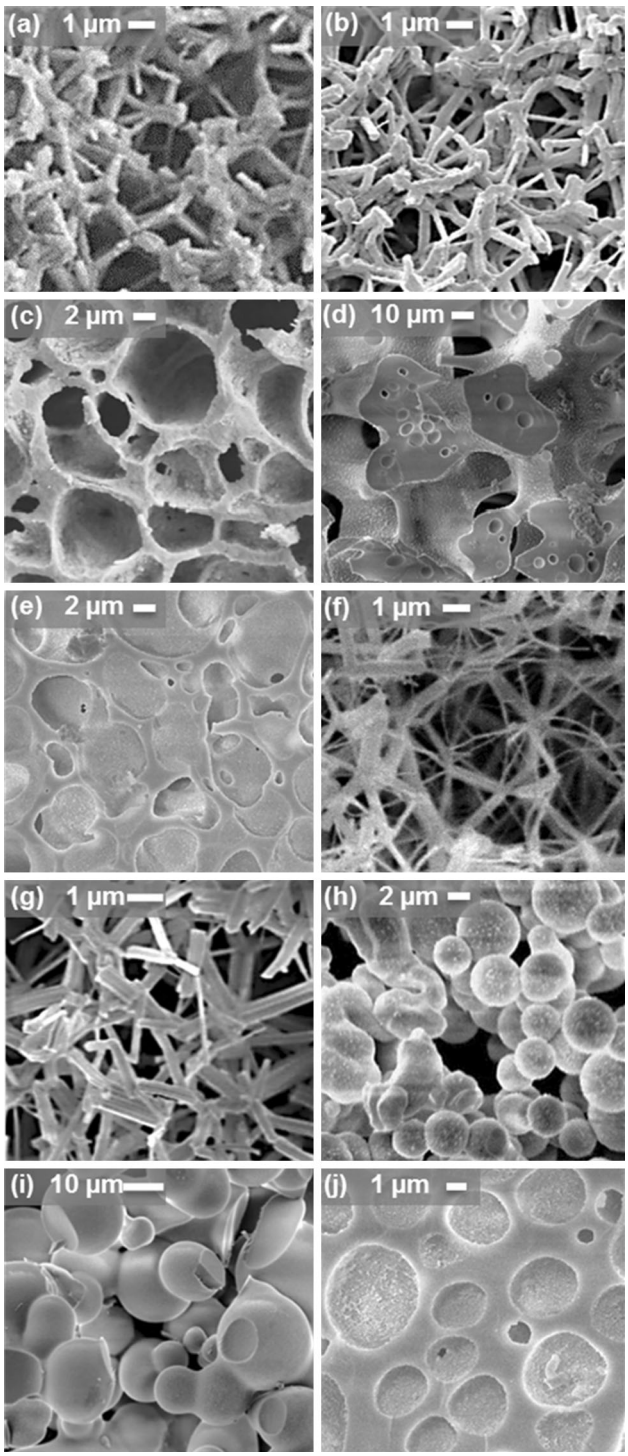

Fig. 2 SEM images of the silica monoliths synthesized with EGMS or TMOS with different acids: **a** EGMS/HCl, **b** EGMS/H_2SO_4, **c** EGMS/HNO_3, **d** EGMS/HBr, **e** EGMS/CH_3COOH, **f** TMOS/HCl, **g** TMOS/H_2SO_4, **h** TMOS/HNO_3, **i** TMOS/HBr, **j** TMOS/CH_3COOH

diameters up to 10 µm can be observed when applying nitric acid. For the gels synthesized with TMOS and HCl, a cellular, very delicate macroporous network with strands of different diameters is obtained compared to the sample with EGMS. This appears to change into thicker strands (0.2–0.5 µm) using sulfuric acid. The EGMS-based gels synthesized with hydrobromic acid showed a very compact macroporous network with features up to 20 µm in diameter. TMOS and hydrobromic acid leads to large spherical particles up to 20 µm in diameter. The application of acetic acid results in isolated pores in the µm-range for the EGMS- and TMOS-based gels.

Chao et al. [19] have also observed a change in the morphology of SBA-15 materials by applying HCl, H_2SO_4 or HNO_3 at pH = 2. With sulfuric acid silica rods with up to 2–4 µm in length were obtained, shorter rod-like structures resulted with hydrochloric acid and more particulate structures together with rods of ~1 µm in length were visible when nitric acid was used. This change was assumed to be a result of the presence of the more polarizable anion SO_4^{2-} and its stronger binding strength to the PEO-units of P123 than Cl^- or NO_3^-, which can induce the formation of elongated micelles. This is in good agreement with our results. The anions Br^- and SO_4^{2-} are weaker and better polarisable than Cl^- or NO_3^- for the applied mineral acids. In the EGMS-based gels the dimensions of the morphology in the micrometer regime decrease in the following order: $Br^- > SO_4^{2-} \approx Cl^- > NO_3^- \approx CH_3COO^-$ and can be supposed as a result of the lower anion polarisability and acidic strength. For the TMOS-based gels this trend is not so pronounced.

To exclude a stabilization of the final silica morphology due the presence of remaining anions, elemental analyses have been performed on the calcined materials. For the EGMS-based gels 0.1 wt% SO_4^{2-} and 0.02 wt% Br^- was determined as well as 0.2 wt% SO_4^{2-} and 0.04 wt% Br^- remained in the TMOS-based samples. No Cl^- or NO_3^- ions were detected in the EGMS- and TMOS-based monoliths when HCl or HNO_3 was applied. The higher anion contents (SO_4^{2-} and Br^-) in the samples prepared from TMOS and the resulting structure in the µm-range (compared to the EGMS-based monoliths with better developed macrostructures) lead to the conclusion, that the remaining anions in the silica network have no positive effect on the network development on a µm-scale.

Figure 3 shows the nitrogen sorption isotherms of the silica samples. The isotherms for the samples prepared with HCl, H_2SO_4 and HNO_3 can be classified as type IV for mesoporous materials with H2 hysteresis. The H2 hysteresis loop is more pronounced when hydrobromic or acetic acid are used, which is an indication of the presence of ink-bottle pores or multimodal pore sizes in the materials [32]. The nitrogen sorption isotherms show an increase of adsorbed nitrogen after filling of the mesopores between $p/p^0 = 0.9–0.99$, except for TMOS/P123/HBr, indicating a macroporous network. This is in good agreement with the SEM-images. From the adsorption/desorption isotherms

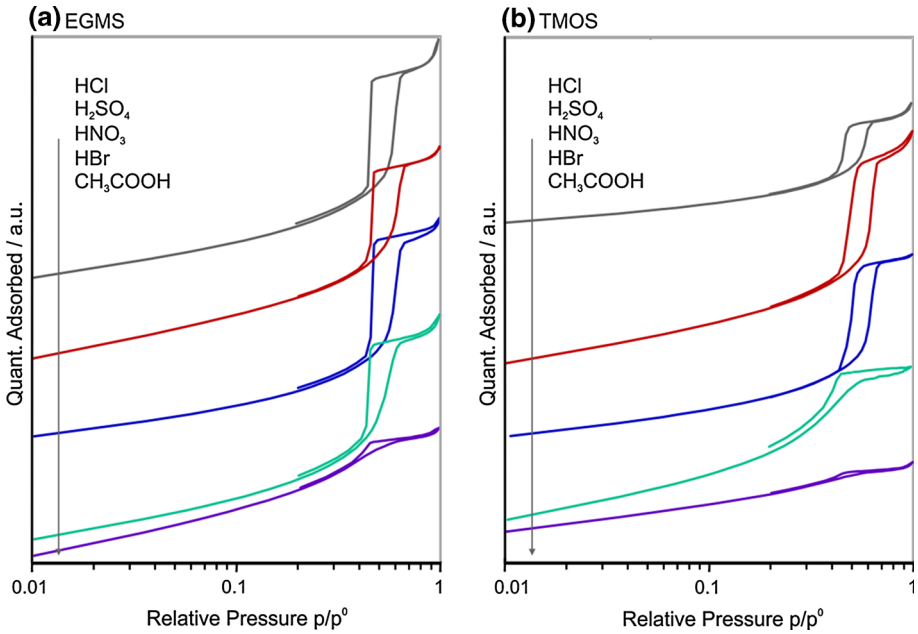

Fig. 3 Adsorption/desorption isotherms of the silica samples synthesized with **a** EGMS or **b** TMOS. The curves are *vertically* shifted for clarity

the specific surface areas (S_{spec}) are calculated and summarized in Table 1. Furthermore parameters, such as adsorbed N_2-volume at $p/p^0 = 0.99$ (V_{max}), mesopore volume in the range of 0.6–0.9 p/p^0 (V_{meso}), initial adsorbed volume at $p/p^0 = 0.01$ (V_0) and mesopore size (d_{ads}) are summarized in Table S1 in the ESI.

For EGMS and sulfuric acid a specific surface area of 641 $m^2\ g^{-1}$ is obtained. Similar specific surface areas were detected for EGMS (634 $m^2\ g^{-1}$) and TMOS (584 $m^2\ g^{-1}$) applying acetic acid, which result from the high amount of micropores in the monoliths. TMOS leads to lower specific surface areas of 320 $m^2\ g^{-1}$ with hydrochloric acid compared to EGMS (464 $m^2\ g^{-1}$) due to a loss in mesopore volume. Remarkably, high specific surface areas of 882 and 787 $m^2\ g^{-1}$ are observed for TMOS with HBr or H_2SO_4, respectively, which is a result of the high micro- as well as mesopore content in the materials.

Figure 4 shows the small angle X-ray scattering (SAXS) curves for the silica samples synthesized from EGMS (a) and TMOS (b). For hydrochloric acid, sulfuric acid and nitric acid long range ordered 2D hexagonally arranged mesopores for both Si-precursor systems are obtained. This is in good agreement with previous works by Chao et al. [19], who showed that the counter ions chloride, sulfate and nitrate had nearly no influence on the 2D hexagonal pore arrangement of SBA-15 materials. In our case, the long range order of the 2D hexagonal lattice is obvious for TMOS-based gels as one can distinguish the first four Bragg reflections (10), (11), (20) and (21) from which the respective lattice d-spacings d_{10}, d_{11}, d_{20} and d_{21} can be calculated. For EGMS samples the scattering peaks are also well pronounced exhibiting the (10), (20) and (21) reflections. The visible intensities in the scattering curves arise from the interplay between the form and structure factor [33]. While the structure factor determines the positions at which peaks appear, the respective peak heights are modulated by the form factor. Although, the form factor is the same for the EGMS as well as for the TMOS sample due to the same diameters of the cylindrical pores, the extinction of the (11) peak for the EGMS sample is observed. This can be explained by the larger d-spacing of the EGMS sample. In this case, all peaks shift towards smaller q-values. At a certain position (where the form factor has its first minimum) the peak intensity is decreased to zero and thus not visible in the scattering intensity.

Fitting of the scattering curves was performed with a Lorenzian profile to determine the peak position q of the most pronounced reflection (Table 1). The first peak position q_{10} gives access to the d-spacing d_{10} and lattice constant a of the 2D hexagonal lattice. Since the (10) reflection is strongly broadened for the samples with HBr or CH_3COOH no appropriate fit was possible. From the adsorption branch of the nitrogen sorption measurements pore size distributions were calculated with the BJH method in order to obtain the mesopore sizes. With $t_{wall} = a - d_{ads}$ the thickness of the silica walls in the materials could be estimated. All calculated parameters for the 2D hexagonal lattice are presented in Fig. 5. For both precursors a slight peak shift towards smaller q-values and therefore larger d_{10} is observed with sulfuric acid instead of hydrochloric or nitric acid.

This results in a d_{10}-spacing of 9.4 nm and a lattice constant of 10.8 nm for EGMS, and $d_{10} = 8.7$ nm and $a = 10.1$ nm for TMOS. Smaller d_{10}-spacings and lattice

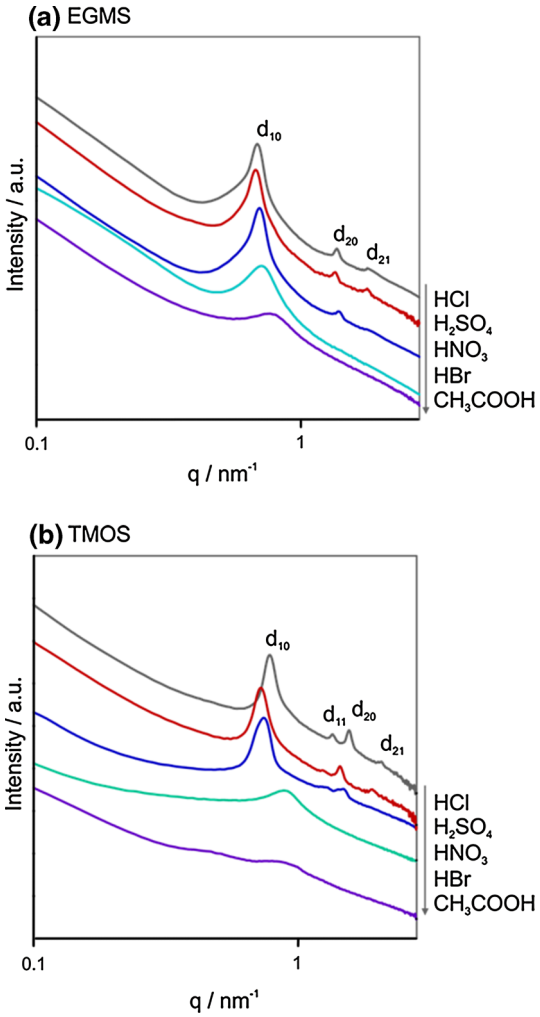

Fig. 4 Small angle X-ray scattering curves of the silica monoliths synthesized with **a** EGMS or **b** TMOS. The curves are *vertically* shifted for better clarity

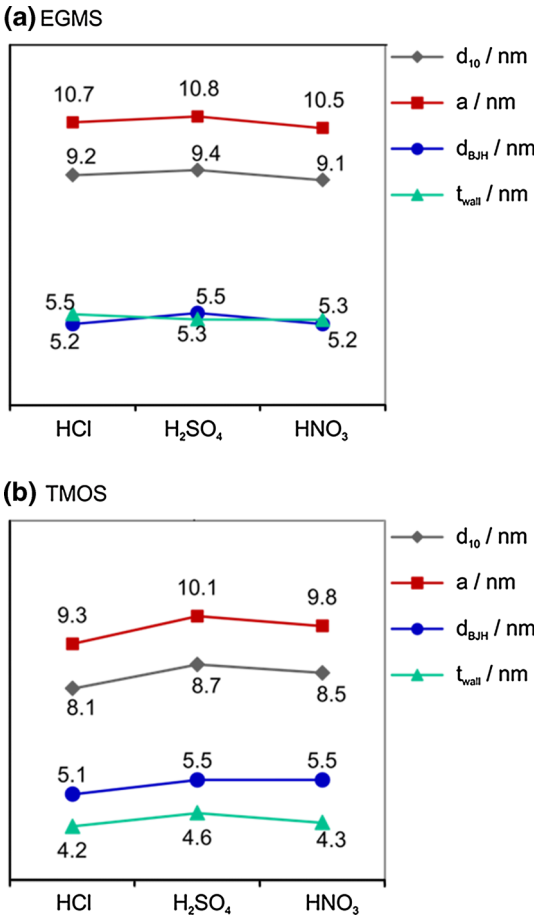

Fig. 5 Structural parameters, such as d_{10}, a, d_{ads}, t_{wall}, of the silica samples synthesized with **a** EGMS or **b** TMOS. (*lines* are drawn for clarity)

parameters are obtained with TMOS as a precursor compared to EGMS. Pore size distributions show no significant differences between EGMS- or TMOS-based gels whether HCl, H_2SO_4 or HNO_3 is used. These materials exhibit mesopore structures with diameters of 5.1–5.5 nm. Due to the smaller lattice parameter of the TMOS samples compared to EGMS but similar mesopore sizes for both precursors, thinner silica walls of 4.2–4.6 nm are obtained with TMOS. For EGMS, silica walls of 5.2–5.3 nm in thickness have been calculated.

Previous experiments with EGMS/P123/HCl (30 wt% surfactant) by Brandhuber et al. [21] have shown that the HCl concentration has a major influence on the 2D hexagonal mesopore arrangement. For different acid concentrations, ranging from 0, 10^{-3}, 10^{-2} to 5 mol L^{-1}, an increase in the long-range order of the mesopore arrangement was observed with increasing HCl content up to 10^{-2} mol L^{-1} at a constant amount of EGMS. However, at very high HCl concentrations (5 mol L^{-1}) the ordered mesoporous network could not be preserved anymore. At this pH, the silica content had to be increased in order to achieve a long-range ordering of the mesopores. Silica monoliths synthesized with EGMS and P123/HCl = 20/80 wt% showed the most pronounced degree of long-range order of the mesopores between a pH of 0 and 2 [31]. However, for the samples with EGMS or TMOS and hydrobromic acid (containing acetic acid) or acetic acid synthesized at pH 0–1.5, at which an ordered mesopore formation should be possible as mentioned above, a collapse of the 2D hexagonally arranged mesopore network with only short-range ordering is observed. This can be assumed as a result of the low acidic strength of the acetic acid, which is additionally lowered in presence of alcohols [18].

Manet et al. [20] observed an influence of the anions, such as SO_4^{2-}, PO_4^{3-}, Cl^-, Br^- and NO_3^-, on the long-range order of the 2D hexagonally arranged mesopores of

SBA-15. The applied anions SO_4^{2-}, PO_4^{3-} and Cl^- are classified as salting-out anions, whereas Br^- and NO_3^- are classified as salting-in anions according to the Hofmeister series [34]. This classification resulted from solubility experiments with different proteins in biological systems and similar trends were also observed for ionic as well as non-ionic surfactants [34–36]. With salting-out anions decreasing protein/surfactant solubility and with salting-in anions increasing protein/surfactant solubility was observed. In-situ SAXS measurements during the synthesis of SBA-15 materials revealed that the salting-out anions (SO_4^{2-}, PO_4^{3-}, Cl^-) were only weakly bond to the surfactant micelles, allowing the silica species to interact with the micelles and highly ordered mesostructured silica materials were obtained. In contrast, the salting-in anions (Br^-, NO_3^-) were more strongly bound to the surfactant micelles, hindering the interactions of the silica species with the micelles and poorly ordered mesoporous silica systems resulted. This is in good agreement to our results for the anions SO_4^{2-}, Cl^- (salting-out) and Br^- (salting-in). However, the results obtained with HNO_3 are different from that reported for SBA-15 [20]. The acetate is classified as a salting-out anion (decreasing salting-out effect: $SO_4^{2-} > CH_3COO^- > Cl^-$ [34]) and a long-range ordering of the mesopores should be possible, but has not been obtained. This is an additional indication that all parameters, such as kind of acid and anion, acidic strength, concentration, influence the formation of the mesostructure in the final materials.

The best developed network with periodically, co-continuous macropores and 2D hexagonally arranged mesopores were obtained with sulfuric acid for both precursors (EGMS or TMOS). In the suggested $(S^0H^+)(X^-I^+)$ mechanism the sulfate anion, with two negative charges, could compensate the positive charges of the silica and surfactant better than single charged ions. Furthermore, sulfate ions bound only weakly to the surfactant micelles allowing for positive interactions of the silica species with the micelles and well-developed long-range ordered silica networks were obtained.

4 Conclusion

Hierarchically organized silica monoliths from either EGMS or TMOS were prepared. Pluronic® P123 served as structure-directing agent. Different acids, such as hydrochloric acid, sulfuric acid, nitric acid, hydrobromic acid and acetic acid, were applied in order to investigate the influence of the acid on macro- and mesopore formation in the final materials. It was possible to show that with HCl or H_2SO_4 both precursors led to monolithic silica samples bearing macro- and mesopores, whereby a bimodal pore size distribution resulted. Moreover, a highly regular network with 2D hexagonally arranged mesopores in the nm-range and a cellular, rod-like macroporous structure in the µm-regime was obtained.

Various synthesis parameters, such as the choice of precursor, surfactant content as well as acid concentration, acid strength and kind of anion influence the formation of the final network. In general, for a given precursor and surfactant content, in a pH range of 0–2 the preparation of macro-/mesoporous silica monoliths is possible. Within this pH-range the acid strength and nature of the anion is important and should be considered in the synthesis of silica materials. Well-developed structures in the µm-regime with co-continuous macropores are observed for the strong acids HCl and H_2SO_4. A lower influence with respect to the kind of acid used was observed for the mesopore arrangement. For both silica precursors a long-range ordered mesopore arrangement was obtained when HCl, H_2SO_4 or HNO_3 was applied, which was lost with hydrobromic and acetic acid.

Acknowledgments S. F. and N. H. acknowledge the Deutsche Forschungsgemeinschaft (Proj. No. HU 1427/5-1) for financial support. J. A. and H. P. acknowledge the Deutsche Forschungsgemeinschaft (Proj. No. PE 1732/1-2) and the Austrian Science Fonds FWF (Proj. No. I449) for financial support.

References

1. Sing KSW, Everett DH, Haul RAW, Moscou L, Pierotti RA, Rouquerol J, Siemieniewska T (1985) Pure & Appl Chem 57:603–619
2. Schüth F (2003) Angew Chem Int Ed 42:3604–3622
3. El-Safty S (2008) J Porous Mater 15:369–387
4. Kresge CT, Leonowicz ME, Roth WJ, Vartuli JC, Beck JS (1992) Nature 359:710–712
5. Thomas B, Baccile N, Masse S, Rondel C, Alric I, Valentin R, Mouloungui Z, Babonneau F, Coradin T (2011) J Sol–Gel Sci Technol 58:170–174
6. Viau L, Néouze MA, Biolley C, Volland S, Brevet D, Gaveau P, Dieudonné P, Galarneau A, Vioux A (2012) Chem Mater 24:3128–3134
7. Huo Q, Margolese DI, Ciesla U, Demuth DG, Feng P, Gier TE, Sieger P, Firouzi A, Chmelka BF (1994) Chem Mater 6:1176–1191
8. Hoffmann F, Cornelius M, Morell J, Fröba M (2006) Angew Chem Int Ed 45:3216–3251
9. Nakanishi K (1997) J Porous Mater 4:67–112
10. Smått J-H, Schunk S, Lindén M (2003) Chem Mater 15:2354–2361
11. Inayat A, Reinhardt B, Uhlig H, Einicke WD, Enke D (2013) Chem Soc Rev 42:3753–3764
12. Petkovich ND, Stein A (2013) Chem Soc Rev 42:3721–3739
13. Nakanishi K, Amatani T, Yano S, Kodaira T (2008) Chem Mater 20:1108–1115
14. Sattler K, Hoffmann H (1999) Prog Colloid Polym Sci 112:40–44
15. Hüsing N, Raab C, Torma V, Roig A, Peterlik H (2003) Chem Mater 15:2690–2692

16. Brook MA, Chen Y, Guo K, Zhang Z, Brennan JD (2004) J Mater Chem 14:1469–1479
17. Dong H, Brennan JD (2006) Chem Mater 18:4176–4182
18. Brinker CJ, Scherer GW (1990) Sol-Gel, The Physics and Chemistry of Sol-Gel ProcessingScience. Academic Press, New York
19. Chao MC, Chang CH, Lin HP, Tang CY, Lin CY (2009) J Mater Sci 44:6453–6462
20. Manet S, Schmitt J, Impéror-Clerc M, Zholobenko V, Durand D, Oliveira CLP, Pedersen JS, Gervais C, Baccile N, Babonneau F, Grillo I, Meneau F, Rochas C (2011) J Phys Chem B 115:11330–11344
21. Brandhuber D, Torma V, Raab C, Peterlik H, Kulak A, Hüsing N (2005) Chem Mater 17:4262–4271
22. Mehrotra R, Narain R (1967) Indian J Chem 5:444–448
23. Hüsing N, Schubert U (1998) Angew Chem Int Ed 37:22–45
24. Brandhuber D, Hüsing N, Raab CK, Torma V, Peterlik H (2005) J Mater Chem 15:1801–1806
25. Soni SS, Brotons G, Bellour M, Narayanan T, Gibaud A (2006) J Phys Chem B 110:15157–15165
26. Brunauer S, Emmett PH, Teller E (1938) J Am Chem Soc 60:309–319
27. Barrett EP, Joyner LG, Halenda PP (1951) J Am Chem Soc 73:373–380
28. Zhao D, Huo Q, Feng J, Chmelka BF, Stucky GD (1998) J Am Chem Soc 120:6024–6036
29. pKa Table (2005) Ripin DH, Evans DA, Washington.depts.washington.edu/eooptic/linkfiles/evans_pKa_table.pdf. Accessed 25 Mar 2014
30. Fritscher C (2008) Self-assembly, hierarchical structure and mechanical properties of (Organo-)silica monoliths. PhD thesis, Vienna University of Technology, Vienna
31. Hartmann S (2009) Hierarchically organized (hybrid) silica monoliths for the application as stationary phases in HPLC. PhD thesis, University of Ulm, Ulm
32. Kruk M, Jaroniec M (2001) Chem Mater 13:3169–3183
33. Smarsly BM, Mascotto S, Weidmann C, Kaper H (2010) Chem Ing Tech 82:823–828
34. Leontidis E (2002) Curr Opin Colloid Interface Sci 7:81–91
35. Alexandridis P, Holzwarth JF (1997) Langmuir 13:6074–6082
36. Kabalnov A, Olsson U, Wennerstroem H (1995) J Phys Chem 99:6220–6230